Available online at www.sciencedirect.com
SCIENCE DIRECT®
Journal of Nuclear Materials 328 (2004) 243–248
journal of nuclear materials
www.elsevier.com/locate/jnucmat

Experiments, characterizations and analysis of a U_3Si_2–Al dispersion fuel plate with sandwich structure

Xi-Shu Wang [a,*], Yong Xu [b]

[a] Department of Engineering Mechanics, Tsinghua University, Beijing 100084, PR China
[b] Institute of Nuclear Energy Technology, Tsinghua University, Beijing 100084, PR China

Received 7 August 2003; accepted 23 April 2004

Abstract

The mixed U_3Si_2–Al fuel is a recently developed dispersion fuel structural material adopted in research reactors. The processing method affects strongly the mechanical properties of the dispersion fuel plate, especially, the fatigue properties, which are of great significance for the reliability and performance of fuel elements in most reactors. The fatigue cracks initiation and propagation processes of the U_3Si_2–Al dispersion fuel plate with sandwich structure were studied in the present paper by in situ SEM observation. The factors influencing fatigue cracks were analyzed, and the nucleation mechanism was proposed. These results indicated that the fatigue crack originated at the vicinal meat edges and propagated primarily along the fuel meat before fracture. The observed fatigue behaviors can be well described by two fracture modes, namely the Mode I and the mixed mode I–II.

1. Introduction

Fatigue crack initiation is one of the most important stages in the fatigue fracture processes of most metals and structural materials. A large number of metallographic experiments have been carried out to elucidate the microscopic physical mechanisms responsible for crack nucleation (see, e.g., [1,2] for review). The present paper examines the nucleation and propagation of dispersion fuel plates with sandwich structure. The sites of crack initiation depend closely on the micro-structural characteristics of the fuel plates and the types of applied stresses. For example, the strength and cracking of a U_3Si_2–Al dispersion fuel plate with aluminum cladding depend strongly on their rolled and heat treated processes [3]. It has been well established that micro-structural defects significantly affect fatigue crack initiation [4–8]. Among possible sites of crack initiation, the slip band is preferred for some multiphase metals under a low cyclic strain. The cyclic strain is concentrated along the slip band and extrusion or intrusion accompanies it [9].

Dispersion U_3Si_2–Al fuel plates with sandwich structure, were produced by Nuclear Material Institute (NMI) and have been used in some research reactors in China and some other countries [10]. Wiencek [11] summarized the efforts of the fabrication technology section at Argonne National Laboratory in the program of Reduced Enrichment Research and Test Reactors (RERTR) during 1978–1990. These researches indicated that the fabrication of the fuel plate was the key aspect of fuel elements production, as shown in Fig. 1. Its quality directly affects the safety and reliability of the fuel elements, especially the fuel plate's dynamic/fatigue properties because the fuel plate is usually subjected to cooling water impaction during their service. The fuel plates may also be subjected to the lower thermal–mechanical cyclic stresses at the higher cycles, or the impacted stress at lower cycles in actual service [12–18].

* Corresponding author. Tel.: +86-10 627 92972; fax: +86-10 627 81824.
E-mail address: xshwang@tsinghua.edu.cn (X.-S. Wang).

0022-3115/$ - see front matter © 2004 Elsevier B.V. All rights reserved.
doi:10.1016/j.jnucmat.2004.04.332

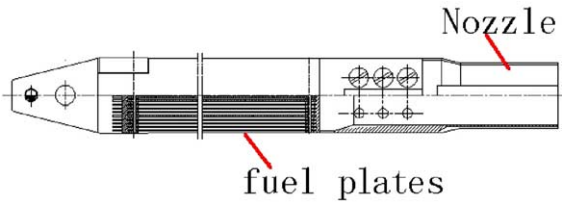

Fig. 1. The fuel plate elements assembled scheme.

In addition, brittle fatigue fracture may occur in fuel plates because their elongation is lower than 3.5% [3]. However, investigations on the fatigue performance of fuel plates with sandwich structure are as yet very limited. Therefore, it seems to be interest to investigate the fatigue behavior of dispersion U_3Si_2–Al fuel plates with sandwich structure. In this paper, fatigue tests were performed using in situ SEM to assess the fatigue crack initiation mechanism and to evaluate the fracture mechanism of fuel plates. This investigation is aimed to establish the relationship between microscopic structure and macroscopic properties of the used fuel plate, and to construct high-performance fuel plate in future.

2. Preparation of material and experimental method

The samples used in these fatigue tests were the U_3Si_2–Al dispersion fuel plates with sandwich structure. The specimens were of flat dog-bone shape with a 20 mm gage length and a 1.38 mm × 2.50 mm gage cross-sections, as shown in Fig. 2. The preparations of the fuel plate began with the dispersion of U_3Si_2 particles in aluminum powder, and were compounded into a U_3Si_2–Al fuel meat. The U_3Si_2 particles and aluminum powder were prepared by casting and repetitively milling/rolling processes to form a meat plate, for which the meat thickness is about 0.60 mm. Then, the U_3Si_2–Al meat was put into the cladding frame of 6061-Al alloy, soldered and rolled repeatedly, and then blister tested at 485 °C for 50 min to obtain good mechanical properties of fuel plate and compatibility between the fuel particles and Al matrix, the fuel meat and cladding of 6061-Al alloy. This procedure resulted in a fuel plate with sandwich structure similar to that reported in Ref. [17,18]. The compatibility between the fuel meat and cladding is the most important factor for any fuel system. It is particularly important to learn about the reaction conditions of the fuel particles with Al matrix when fuel particles directly contacts with Al matrix in U_3Si_2–Al. When the rolled fuel plate was dissected under typical technological conditions [18], a slight reaction surrounding the U_3Si_2 particles between fuel particles and Al matrix were observed and the formed reaction zone can be observed on the fracture surface. If the temperature of heat treatment was over 600 °C, U_3Si_2 particles in the fuel plate rapidly reacted with Al. The reaction product was also be determined to be UAl_x by the X-ray diffraction (XRD) powder photographical technique. To observe the small fatigue cracking of fuel plate with sandwich micro-structure clearly, the observation faces of the samples were carefully polished prior to fatigue testing. All fatigue crack initiation and propagation tests were performed in the vacuum chamber of the SEM using the specially designed servo-hydraulic testing system designed by Shimadzu Inc., which provides pulsating (sine wave) loading. The load frame has a load capacity of 10 ± 1 kN and displacement range of ±25 mm. In the test conditions, the microscopy was operated in a high vacuum state (pressure range at the electron gun to 10^{-4} Pa) at a 15 kV accelerating voltage. All fatigue tests were by force controlled at a stress ratio of $R = 0.1$ [19–21]. All processes of fatigue crack initiation and propagation were monitored or recorded at a frequency of 0.01 Hz, while the work frequency of fatigue tests was 4 Hz in order to prompt the fatigue damage of the U_3Si_2–Al dispersion fuel plate.

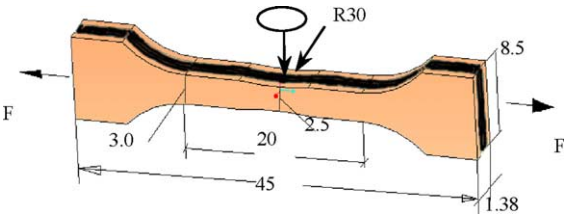

Fig. 2. Geometry of U_3Si_2–Al dispersion fuel plate with sandwich structure.

3. Stress intensity factors along an interface layer

As shown in Fig. 3, the sample of a dispersion U_3Si_2–Al fuel plate with sandwich structure can be approximately considered as two phases: U_3Si_2–Al fuel meat phase and the cladding frame of 6061-Al phase with thickness of b_m (0.6 mm) and b_c (2×0.39 mm). To illustrate the excellent compatibility between the fuel meat and the cladding, the interface layers in these two phases are defined in the fracture surface (Fig. 3). It is clearly seen that the thicknesses of interface layers are not uniform and there are abundant shrinkage voids in these layers. In addition, when the section of sample was subjected to the applied cyclic loading F (or $\sigma_{app.}$), each phase presents in the interface layers subjected to the same strains but different stresses. Therefore, the fatigue crack initiation site can be defined as the weak phase. The stress in the two phases can be expressed as

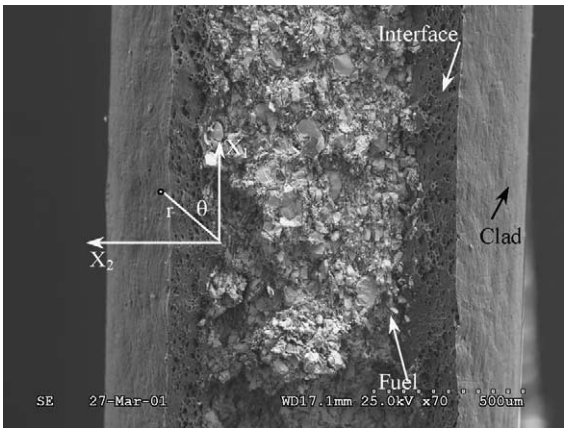

Fig. 3. The fracture section of U_3Si_2–Al dispersion fuel plate.

$$\sigma_m = \frac{E_m}{E}\sigma_{app.}, \quad \sigma_c = \frac{E_c}{E}\sigma_{app.}, \tag{1}$$

where E, E_m, E_c are the Young's modulus of the fuel plate, fuel meat and cladding, respectively. Because the mechanical properties of the phases are different, the higher stress may be induced in the interface layers as the strains are imposed continuously and conformably. Due to the effect of the interface layer on the deformation, the stress in the interface layer should be between σ_m and σ_c. According to interface fracture theory analysis [22,23], the distribution of stress at the tip of an interface crack is expressed in terms of the stress intensity factors. With respect to the coordinate system shown in Fig. 3, the stresses along the x_1-axis at the crack tip are expressed by the K-field

$$\sigma_{22} + i\sigma_{12} = \frac{K_I + iK_{II}}{\sqrt{2\pi r}}\left(\frac{r}{\ell_k}\right)^{i\alpha}, \tag{2}$$

where K_I, K_{II} are the mode-I and II stress intensity factors, respectively, $\sigma_{22} + i\sigma_{12}$ is a complex stress, ℓ_k denotes a reference length to normalize the distance r. α is the bielastic constant given by

$$\begin{aligned} &\alpha = \frac{1}{2\pi}\ln\left[\left(\frac{k_c}{G_c}+\frac{1}{G_m}\right)\Big/\left(\frac{k_m}{G_m}+\frac{1}{G_c}\right)\right],\\ &k_j = 3 - 4v_j \quad \text{(Plane Strain)},\\ &k_j = (3 - v_j)/(1 + v_j) \quad \text{(Plane Stress)}, \end{aligned} \tag{3}$$

where G_m, G_c are the shear modulus of meat and cladding, respectively, and v_j ($j = m, c$) are the Poisson's ratio of meat and cladding, and the subscripts 1 and 2 denote the phase located $x_2 > 0$ and $x_2 < 0$, respectively [24]. We can obtain an absolute value and an argument from Eq. (2) as [24]

$$\begin{aligned} &\text{Absolute value}: \sqrt{\sigma_{22}^2 + \sigma_{12}^2} = \frac{\sqrt{K_I^2 + K_{II}^2}}{\sqrt{2\pi r}},\\ &\text{Argument } \arctan\left(\frac{\sigma_{22}}{\sigma_{12}}\right) = \arctan\left(\frac{K_I}{K_{II}}\right) - \alpha\ln\left(\frac{r}{\ell_k}\right). \end{aligned} \tag{4}$$

The fracture of the interface layer between dissimilar materials depends mainly on this mixed fracture mode as mentioned in other references [24–28]. Therefore, the fracture in the interface layers may occur more readily compared to the fracture of other layer because of the significant effect of boundary layers near the interfaces between the mismatched phases [29].

4. Experimental results and discussions

The images in Fig. 4 show the interface crack morphology involved two interface layers with sandwich structure under different applied maximum stress and cycles. It is clearly seen that the interface crack initiation and propagation were subjected to the applied maximum stresses at $R = 0.1$. The fatigue crack propagating along the cladding (x_2-axis) was not obvious because the plastic deformation of the cladding edge resists the interface crack propagation in the thickness direction. On the other hand, the fatigue crack propagates mainly along the interface layer because the stress component $\sigma_{22} < \sigma_{12}$, as shown in Fig. 4(a)–(d). It was worthy of noting that the interface cracks may nucleate symmetrically at both the sides of the interface layers, as shown in Fig. 4(d). In addition, with the increase in the applied maximum stress at $R = 0.1$, the interface crack propagation direction varies. Evans et al. [30], Feng and Yu [31] pointed out that the cracking characterization in the vicinal interface could be explained by a micromechanics model of shielding of the crack tip due to asperity interaction. The brittle fracture occurred at smashing cleavage of U_3Si_2 particles on the crack path, as shown in Fig. 4(a) and (b). This suggests that the fatigue fracture mechanisms at the micro-scale are rather complicated for the dispersion U_3Si_2–Al fuel plate with sandwich structure. This fracture process depends mainly on the micro-structure of the vicinal interface layer and the ratio of the normal and shear components (σ_{ij}) of the stresses at the crack tip as well as the toughness of the cladding and meat. In addition, the interface crack propagation observed in Fig. 4(d) is not the main reason of fatigue fracture. Nevertheless, it is seen that the interface crack initiation positions are usually at the vicinal meat's interface and that the fatigue crack propagates along the x_1 and x_2 directions under our experimental conditions. Subsequently, the fatigue crack growth along the fuel meat leads to the fatigue fracture of fuel plate.

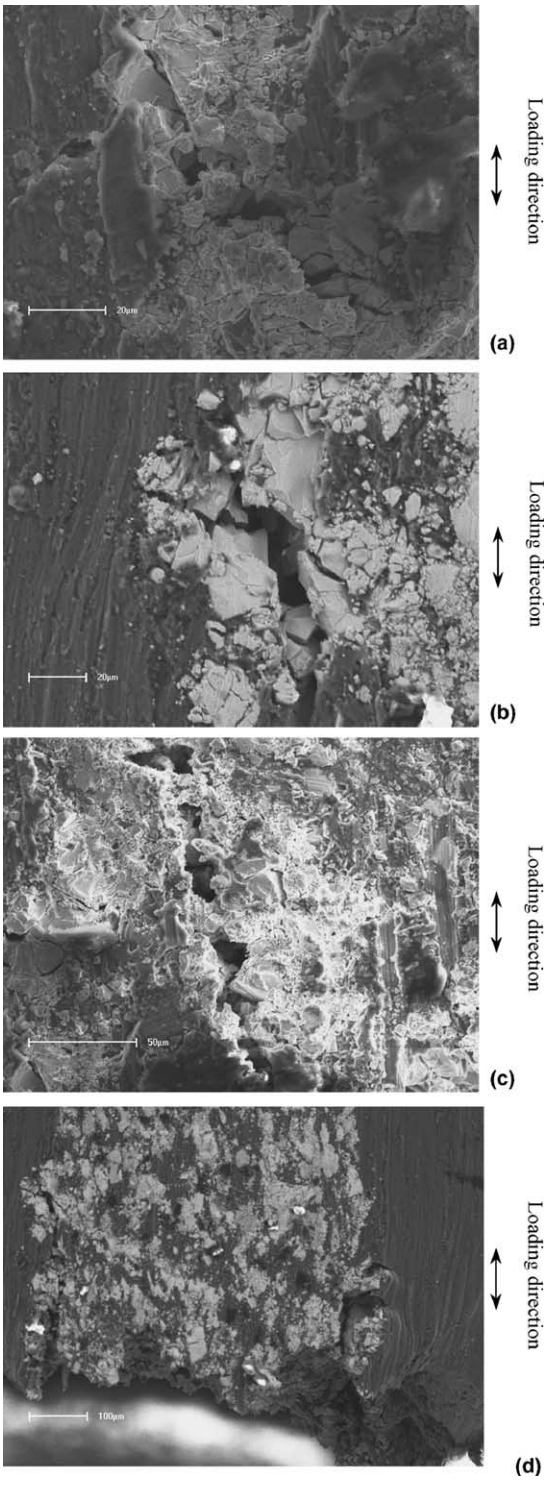

Fig. 4. Interface crack under different applied maximum stress and cycles (a) at $N = 3660$, $\sigma_{max} = 130$ MPa (scale bar is 20 μm); (b) at $N = 16921$, $\sigma_{max} = 120$ MPa (scale bar is 20 μm); (c) at $N = 55217$, $\sigma_{max} = 80$ MPa (scale bar is 50 μm); (d) SEM image under $\sigma_{max} = 80$ MPa (scale bar is 50 μm).

Fig. 5. Cracks and propagation in meat at $N = 21216$, $\sigma_{max} = 100$ MPa (scale bar is 100 μm).

We successfully observed that the fatigue crack propagated along the fuel meat (the x_2 axis direction) under $\sigma_{max} = 100$ MPa after $N = 21216$. The SEM image in Fig. 5 confirms that the fatigue crack originated from the interface layer, and that the fatigue crack growth path is a preferred vertical loading axis in the macroscopic analysis. This is particularly true for the crack in the fuel meat because the fracture of mode I is the main reason of fracture for this fuel plate.

Fig. 6(a) shows the fatigue fracture surface of the dispersion U_3Si_2–Al fuel meat. Many cleavage cracks of U_3Si_2 particles can be found under the cyclic loading. This means that the Mode-I fracture is the primary failure mechanism, for which a tensile force acts parallel to the crack surface in a manner similar to the fracture mechanism of rocks. At the same time, some brittle fracture characters of U_3Si_2 particles surfaces are also easily detectable. The macroscopically flat fracture surface at the fuel meat was irregular at micro-scale and the striations reflected the topography of the U_3Si_2 particle boundaries, the separation of which leads to the brittle particles fracture. As Fig. 6(b) indicates clearly, fractography can also be a useful tool for identifying brittle particles fracture as a failure mechanism.

At micro-scale, the fracture surface of the U_3Si_2 particle is much smoother than that of the cladding, but it is not 'atomistically' smooth. Small ridges, called river striations, can be clearly seen, indicating that that the propagating crack periodically displaces itself vertically up and down by small distances with respect to the 'average' fracture plane. This is caused by the small structural irregularities in the U_3Si_2–Al meat that make it energetically more favorable for the crack occasionally to change its fracture plane in preference to propagating continuously across a surface with perturbed displacements no greater than atomic dimensions. This irregular propagation of a brittle crack also occurs in the dis-

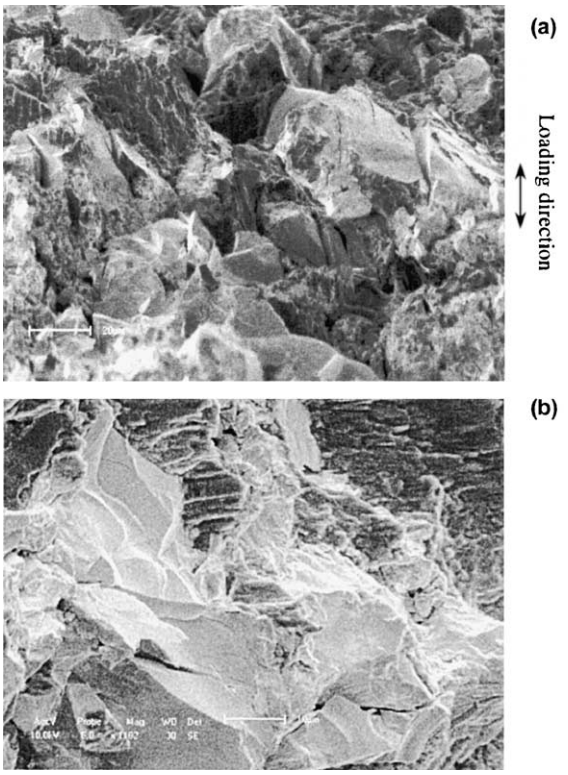

Fig. 6. SEM image of fatigue fracture at the meat center (a) SEM image of fatigue fracture at the meat center. (b) Enlarged image at the meat center (scale bar is 10 μm).

persion U_3Si_2–Al meat, and is evident in the fractograph of Fig. 6(a) and (b).

To examine whether the fatigue fractures of fuel plates are possible to occur during their service, the contracted fatigue tests of two fuel plates were carried out. One of the samples used in the fatigue tests was pretreated at 110 °C, lower stress level (such as a pressed stress amplitude of one MPa), continuously to be vibrated for 1200 h in simulative state, and other samples is original fuel plate. The *S–N* curves as shown in Fig. 7 indicated that there is a difference of curves slopes in these states. This means that the fatigue performance of the original fuel plate will be improved during their service at lower cycles or higher stress levels because the effect of environment in the reactor on the fatigue performance of fuel plate elements plays an important part at higher stress levels such as these elements are subjected to the impacted loading. One of reasons is the elements in the reactor was aged at 110 °C so that their fatigue performance is better relatively without the fuel plates to be aged. However, the improved fatigue performance of the fuel plate during their service is not obvious with increasing of cycles. Contrarily, the fatigue performance of the fuel plate becomes awful at lower stress levels as shown in Fig. 7. The results of *S–N* curves

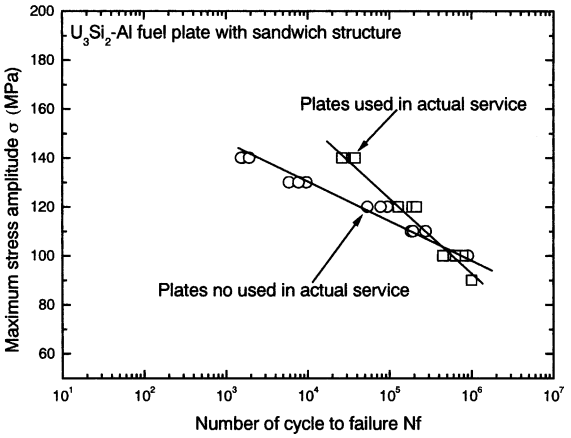

Fig. 7. The *S–N* curves of fuel plates with contracting two states.

indicated that the fuel plate would be accelerated fatigue fracture at lower stress levels as increasing of cycles even if no considering the effect of corrosive fatigue on the fuel plate. As the fuel plate mainly work at 110 °C, lower stress levels and for longer times, it is noteworthy that the effect of fatigue problem on the security and reliability of fuel plate elements during their service.

5. Conclusions

Based on in situ SEM observations of fatigue crack initiation and propagation and fatigue tests on a U_3Si_2–Al dispersion fuel plate with sandwich structure, fatigue failure behaviors at the different stresses levels, at $R = 0.1$, have been analyzed. The following results have been obtained:

(1) Fatigue fracture of a U_3Si_2–Al dispersion fuel plate is not ultimate due to fatigue crack propagation along the interface between the fuel meat and the cladding. The fatigue crack grows mainly along the fuel meat, and finally leads to the fatigue fracture of a U_3Si_2–Al dispersion fuel plate.
(2) The fatigue crack initiation site occurs mainly at the interface layer near the U_3Si_2 particles due to a coupling of mode-I and II fracture.
(3) The symmetrical interface cracks on the dispersion U_3Si_2–Al fuel plate with sandwich structure can be observed in situ SEM in our experimental conditions.
(4) The fatigue crack through the cladding, which consists of the 6061 aluminum alloy, is less preferential because the resistance of fatigue crack propagation of cladding is greater than that of the fuel meat.
(5) The quality of the interface layer formed between the meat and cladding in the rolling process depends

strongly on not only the tensile strength of fuel plate but also the fatigue behavior. The fatigue properties of the fuel plate with sandwich structure can be improved by optimizing the cladding, the U_3Si_2–Al powder composite contents and the process of rolling as well as by improving the heat treatment method.

(6) The fatigue performance of fuel plate during actual service will be improved at lower cycles or higher stress level, but it will become awful at lower stress level as increasing the cycles based on the contrasted fatigue tests.

Acknowledgements

This work was supported by the National Natural Science Foundation of China (Grant Nr.: 90205022).

References

[1] J.C. Grosskreutz, Phys. Stat. Solid (b) 47 (1971) 359.
[2] C. Laird, D.J. Duquette, in: O.F. Devereux, A.J. McEvily, R.W. Staehle (Eds.), Corrosion Fatigue, NACE2, 1972, p. 88.
[3] X.S. Wang, Y. Xu, Appl. Compos. Mater. 10 (2003) 159.
[4] J.M. Hyzak, I.M. Bernstein, The effect of defects on the fatigue crack initiation process in two P/M superalloys: Part I. fatigue origins, AFML-TR-80-4063, Air Force Materials Laboratory, Wright-Patterson AFB, Ohio, 1980.
[5] N.E. Mott, Acta Metall. 6 (1958) 195.
[6] T.H. Lin, Y.M. Ito, J. Mech. Phys. Solids 17 (1969) 511.
[7] S. Kleiner, O. Beffort, A. Wahlen, P.J. Uggowitzer, J. Light Met. 2 (2002) 277.
[8] Q.G. Wang, D. Apelian, D.A. Lados, J. Light Met. 1 (2001) 73.
[9] K. Tanaka, T. Mura, J. Appl. Mech. 48 (1981) 97.
[10] Z.G. Di, Y.B. Guo, China Nuclear Information Centre Atomic Energy Publish (CNIC-01009), 1995, p. 1 (in English).
[11] T.C. Wiencek, Summary report on fuel development and miniplate fabrication for the RERTR program, 1978 to 1990, Argonne national Laboratory, Argonne, Illincis, Operate by the University of Chicago, August, 1995, p. 1.
[12] D.A. Petti, K.A. McCarthy, W. Gulden, S.J. Piet, Y. Seki, B. Kolbasov, J. Nucl. Mater. 233–237 (1996) 37.
[13] A.-A.F. Tavassoli, J. Nucl. Mater. 302 (2002) 73.
[14] US Nuclear Regulatory Commission, US Nuclear Regulatory Commission Report NUREG-1313, 1988.
[15] R.F. Domagala, T.C. Wiencek, H.R. Thresh, in: Proceedings of 1984 RERTR International Conference, 1985, p. 47.
[16] T.C. Wiencek, Argonne National Laboratory Report ANL/RERTR/TM-9, 1988.
[17] R.F. Domagala, T.C. Wiencek, H.R. Thresh, Nucl. Technol. (1983) 62.
[18] J.L. Snelgrove, R.F. Domagala, G.L. Hofman, T.C. Wiencek, G.L. Copeland, R.W. Hobbs, R.L. Senn, Argonne National Laboratory Report ANL/RERTR/TM-11, 1987.
[19] M. Jono, in: X.R. Wu, Z.G. Wang (Eds.), Fatigue'99, Proceedings of the 7th International Fatigue Conference, Beijing, PR China, vol. 1/4, 1999, p. 57.
[20] X.S. Wang, J.H. Fan, J. Mater. Sci. 39 (7) (2004) 2617.
[21] X.S. Wang, X. Lu, H.D. Wang, Mater. Sci. Eng. A 364 (1–2) (2004) 11.
[22] M.D. Thouless, Acta Metall. 38 (1990) 1135.
[23] F. Erdogan, Trans. ASME Ser. E, J. Appl. Mech. 32 (1965) 403.
[24] T. Ikeda, N. Miyazaki, Eng. Fract. Mech. 59 (6) (1998) 725.
[25] J.R. Rice, G.C. Sih, Trans. ASME Ser. E, J. Appl. Mech. 32 (1965) 418.
[26] J.R. Rice, Trans. ASME Ser. E, J. Appl. Mech. 55 (1988) 98.
[27] J.W. Hutchinson, M.E. Mear, J.R. Rice, J. Appl. Mech. 54 (1987) 828.
[28] X.S. Wang, Y. Xu, X.Q. Xu, Appl. Compos. Mater. 11 (3) (2004) 145.
[29] G.F. Wang, S.W. Yu, X.Q. Feng, Mech. Res. Commun. 28 (2001) 87.
[30] A.G. Evans, B.J. Dalgleish, M. Hu, J.W. Hutchinson, Acta Metall. 37 (1989) 3249.
[31] X.Q. Feng, S.W. Yu, Damage Micromechanics of Quasi-Brittle Solids, Higher Education, Beijing, 2002.